

**STATIC AND PULSED REACTIVITY
MEASUREMENTS ON LARGE FUEL FORMS**

by

R. L. Currie
P. B. Parks

Approved by

J. R. Hilley, Research Manager
Experimental Physics Division

September 1971

**E. I. DU PONT DE NEMOURS & COMPANY
SAVANNAH RIVER LABORATORY
AIKEN, S. C. 29801**

*CONTRACT AT(07-2)-1 WITH THE
UNITED STATES ATOMIC ENERGY COMMISSION*

This document was prepared in conjunction with work accomplished under Contract No. AT(07-2)-1 with the U.S. Department of Energy.

DISCLAIMER

This report was prepared as an account of work sponsored by an agency of the United States Government. Neither the United States Government nor any agency thereof, nor any of their employees, makes any warranty, express or implied, or assumes any legal liability or responsibility for the accuracy, completeness, or usefulness of any information, apparatus, product or process disclosed, or represents that its use would not infringe privately owned rights. Reference herein to any specific commercial product, process or service by trade name, trademark, manufacturer, or otherwise does not necessarily constitute or imply its endorsement, recommendation, or favoring by the United States Government or any agency thereof. The views and opinions of authors expressed herein do not necessarily state or reflect those of the United States Government or any agency thereof.

This report has been reproduced directly from the best available copy.

Available for sale to the public, in paper, from: U.S. Department of Commerce, National Technical Information Service, 5285 Port Royal Road, Springfield, VA 22161

phone: (800) 553-6847

fax: (703) 605-6900

email: orders@ntis.fedworld.gov

online ordering: <http://www.ntis.gov/help/index.asp>

Available electronically at <http://www.osti.gov/bridge>

Available for a processing fee to U.S. Department of Energy and its contractors, in paper, from: U.S. Department of Energy, Office of Scientific and Technical Information, P.O. Box 62, Oak Ridge, TN 37831-0062

phone: (865)576-8401

fax: (865)576-5728

email: reports@adonis.osti.gov

CONTENTS

	<u>Page</u>
Introduction	3
Summary	4
Discussion	5
Description of Fuel and Arrays	5
Experimental Procedures	9
Static Measurements	9
Pulsed Measurements	11
Results	13
Appendix A - Reduction of Harmonic Distortion in Pulsed Neutron Measurements	19
Appendix B - Method for Obtaining β_{eff}/β	22
References	23

INTRODUCTION

Safe handling and storage requirements for nuclear fuels usually are based on calculations of the effective multiplication constant, k_{eff} , of arrays of fuel pieces under various conditions of moderation and reflection. Easily enforced procedures can eliminate most potential moderators and reflectors except water. Therefore, safe storage of fuel usually is assured by limiting the number of fuel pieces, their spacing, and/or their dimensions such that the calculated k_{eff} under conditions of complete water immersion does not exceed some limit. For economic reasons, this limit on calculated k_{eff} is generally chosen as high as practical, provided sufficient allowances are made for inaccuracies in the calculations. These inaccuracies may be determined by comparing the calculated and measured reactivities of representative lattices.

Numerous critical measurements have been reported and compared to calculated results for homogeneous solutions.^{1,2} Likewise, measurements on slightly enriched uranium metal and oxide lattices have been reviewed³ and subsequently compared with calculations.⁴ The present subcritical experiments were undertaken to provide reactivity information on arrays of large, highly enriched ^{235}U alloy fuel forms moderated with H_2O to serve as benchmarks for determining the inaccuracies of criticality codes applied to these fuel forms and other similar material.

SUMMARY

The experiments consisted of static (buckling) and pulsed measurements to determine the multiplication constant, k_{eff} , of regular, subcritical arrays of large fuel forms moderated and reflected with H_2O . Two geometric types of fuel forms were used in the tests; both contained 9.985 wt % uranium (92.2% ^{235}U) in aluminum. Results were compared to calculations with the MGBS-TGAN⁵ and KENO⁶ codes. Computations with MGBS-TGAN for arrays of the more massive of the two forms proved conservative in calculating k_{eff} (calculated too large a k_{eff}) by 9-12%; they were 7-7.5% conservative when applied to the second, less massive type. KENO proved more accurate in calculating k_{eff} ($\leq 5\%$ error in k_{eff}) but was not always conservative.

An experiment on a hexagonal array of the second type of form at large spacings showed that MGBS calculates a material buckling for this large pitch which is in error by more than $13 m^{-2}$. This is equivalent to an error of about 4% in k_{eff} .

DISCUSSION

DESCRIPTION OF FUEL AND ARRAYS

The fuel pieces used in the experiments were of two types: bare U-Al alloy castings, and aluminum-clad "logs" extruded from the castings. The U-Al alloy in both cases was 9.985 wt % uranium (92.2% ^{235}U) in aluminum. The dimensions and ^{235}U contents of these two types of forms are given in Table I. The static measurements involved making a vertical flux traverse over a distance in excess of one meter to obtain the desired accuracy. The logs were extruded to 111.8 cm as a single unit; the castings were stacked six to the column around an 11.2-cm-OD, 10.8-cm-ID aluminum tube to obtain a height of 113 cm. (The castings each had a 20° inside taper on one end, and a 20° outside taper on the other. This accounts for the fact that the stacked column height was less than 6 times a single unit length.)

In most of the experiments the forms were arranged in rectangular arrays of various sizes. A rigid aluminum support frame maintained accurate spacing within the arrays. (The support frame is shown in Figure 1 loaded with a 2 x 3 array of stacks of castings.) During the experiments, the loaded support frame was flooded with water to the top of the fuel; the H_2O surrounding the open support structure then approximated a 100% H_2O reflector on the sides and bottom.

TABLE I
Fuel Forms Used in Experiments

Form	Dimensions, cm				Total Length	kg $^{235}\text{U}/\text{ft}$
	ID Cladding	ID Fuel Alloy	OD Fuel Alloy	OD Cladding		
Casting		11.21	20.07		20.3	1.94
Log	10.07	10.22	12.12	12.27	111.8	0.297

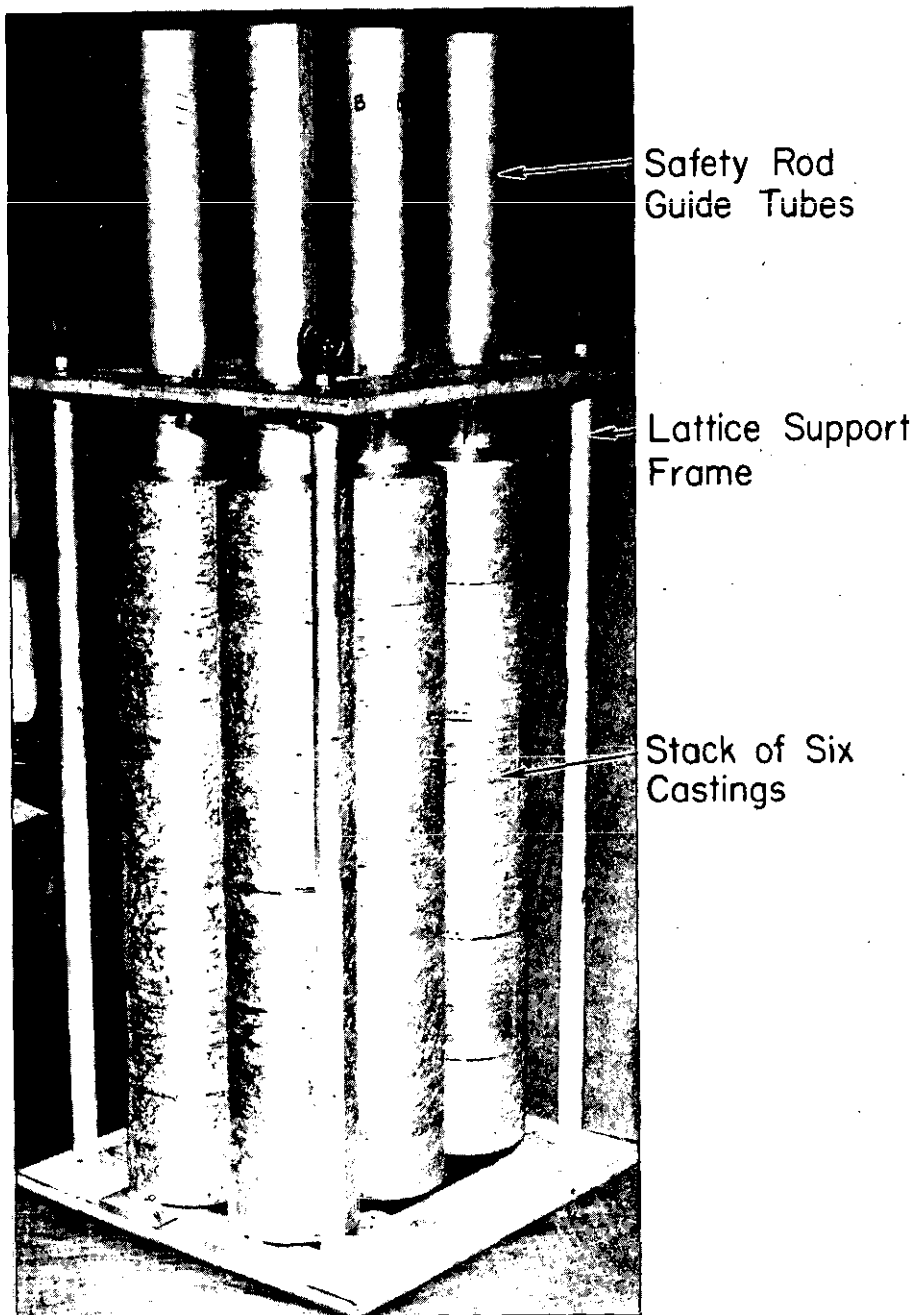


FIG. 1 LATTICE SUPPORT FRAME WITH 2X3 ARRAY OF CASTINGS

One set of measurements was made with 37 logs at wide spacing (7-in. triangular pitch) to determine the applicability of the codes to this geometry and to extend the measurements well beyond the maximum reactivity configuration. In addition, the material buckling of the array was measured directly. For these experiments, the logs were suspended vertically on 1/2-in. central aluminum rods from the SE grid beam system in the hexagonal pattern shown in Figure 2.

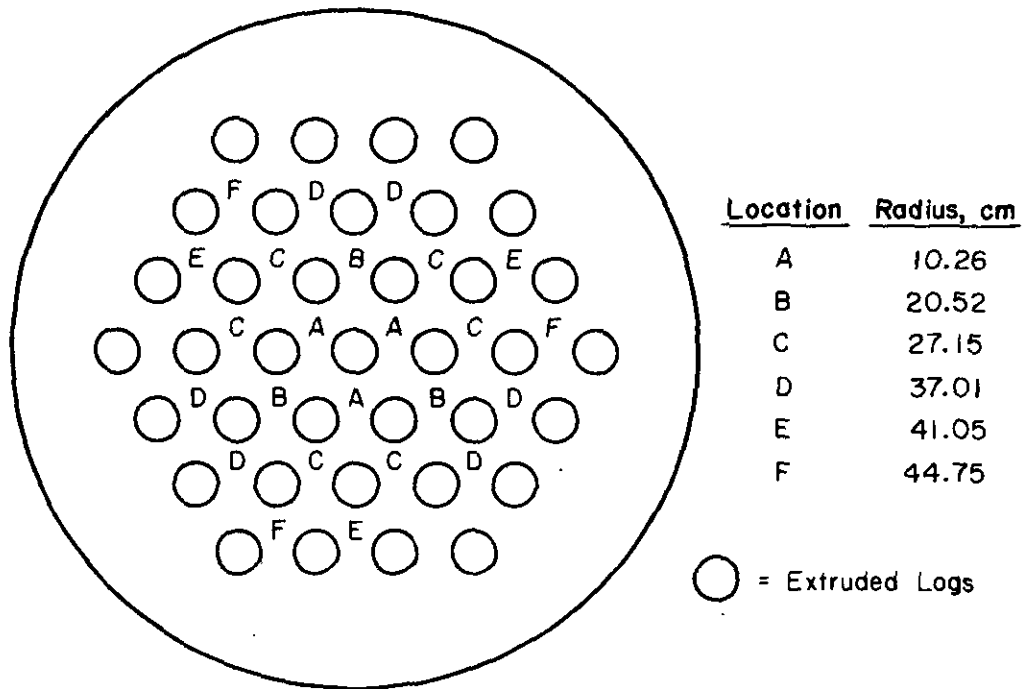


FIG. 2 GOLD PIN TRAVERSE LOCATIONS IN 37 LOG EXPERIMENTS

All experiments were conducted in the Subcritical Experiment (SE) facility⁷ (Figure 3), a cadmium-wrapped aluminum tank 152 cm in diameter and 213 cm high. The SE is centered above the Standard Pile (SP),⁸ which serves as a neutron source. The SP is a 152-cm cube of graphite with a light-water-cooled core of ^{235}U -Al fuel. The facilities are coupled through a cylindrical graphite pedestal, which minimizes spatial harmonics in the cylindrical SE from the cubical source reactor.

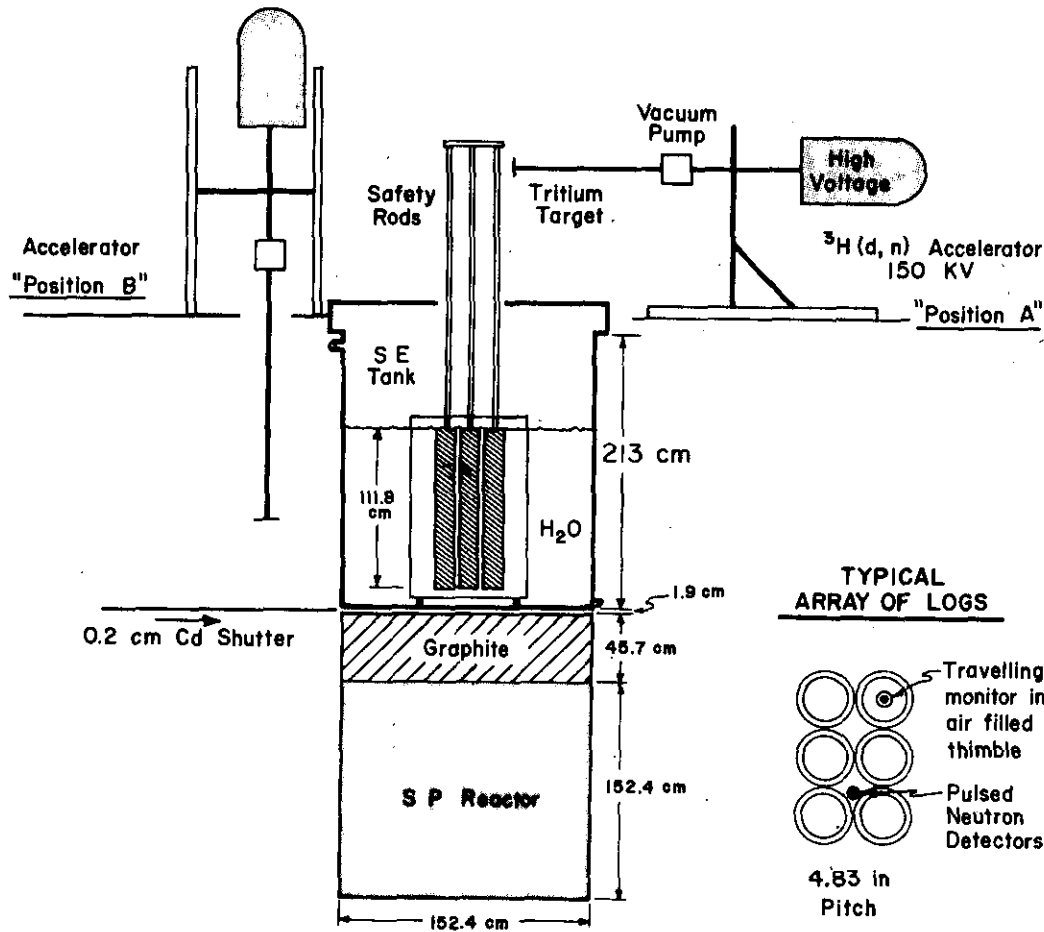


FIG. 3 EXPERIMENTAL ARRANGEMENT

EXPERIMENTAL PROCEDURES.

Static Measurements

In the static measurements the multiplication constants of individual arrays were obtained by determining the material bucklings of the arrays and using a one-group formula to convert these results to appropriate values of k_{eff} . The material buckling was obtained from the expression

$$B_m^2 = B_r^2 - \kappa^2 \quad (1)$$

where B_r^2 is the transverse geometric buckling, and κ is the inverse relaxation length.

In the rectangular array measurements, κ was determined from axial flux traverses obtained with a small, boron-lined, gamma-compensated ion chamber driven at a constant speed.⁹ Digitized current readings from the chamber were recorded at 2-cm axial intervals. The axial flux traverses were repeated for each array after interposing a cadmium shutter between the pedestal and the bottom of the SE tank. Axial flux profiles free from the background effect of extraneous neutron sources, such as fast neutrons from the reactor, were obtained as the difference between the results of the shutter-out and shutter-in measurements.

The SE profiles were then fitted to analytic functions by a least squares analysis code, and a value for κ was obtained. For lattices in which κ^2 is positive (i.e., $B_r^2 > B_m^2$), the flux shape is described by the relation

$$\phi(Z) = A \sinh \kappa(Z + \delta)$$

where

$A = \text{constant}$

$Z = \text{distance below moderator surface}$

$\delta = \text{extrapolation distance in air}$

For lattices sufficiently close to critical that κ^2 is negative (i.e., $B_r^2 < B_m^2$), the axial flux shape is represented by the expression

$$\phi(Z) = A \sin \kappa(Z + \delta)$$

B_r^2 for rectangular arrays is given by the standard expression

$$B_r^2 = \left(\frac{\pi}{N_x P_x + 2\delta_x} \right)^2 + \left(\frac{\pi}{N_y P_y + 2\delta_y} \right)^2 \quad (2)$$

where

N_i = number of assemblies in the i^{th} direction

P_i = center-to-center spacing in the i^{th} direction

δ_i = extrapolation distance in the i^{th} direction

The transverse dimensions of the rectangular arrays were so small that measurement of extrapolation distances was impossible; calculated values were utilized instead.

For the 37 log experiment, gold pins were suspended at the locations shown in Figure 2. Standard activation, counting, and data reduction procedures were used to give relative activations at seven elevations for each of the six radii. Data from the asymptotic region (defined as having a constant neutron spectrum versus position as determined with Cd ratio measurements) were fit to J_0 and sinh functions to give measured values for both B_r^2 and κ^2 . Equation (1) was then used to determine a value of B_m^2 .

Using the one-group diffusion approximation,

$$k_{\text{eff}} = \frac{1 + M^2 B_m^2}{1 + M^2 B_g^2} \quad (3)$$

where M^2 is the migration area for the lattice, and B_g^2 is the total geometric buckling. From Equation (1) and the definition of B_g^2 , a k_{eff} (static) can be defined by

$$k_{\text{eff}} \text{ (static)} = \frac{1 + M^2 (B_r^2 - \kappa^2)}{1 + M^2 (B_r^2 + B_z^2)} \quad (4)$$

where B_z^2 is the axial geometric buckling. Calculated values of M^2 and B_z^2 , with appropriate values of κ^2 and B_r^2 , can then be used in Equation (4) to produce a k_{eff} (static) for any lattice. This k_{eff} (static) is the parameter reported for each lattice.

Under the assumption that Equation (4) is directly applicable to the small system considered here, the deviation of k_{eff} (static) from the actual multiplication constant of the array depends primarily on the accuracy of the calculated parameters. Since the axial dimension is in excess of one meter, errors in the total geometric buckling due to inaccuracies in the assumed axial extrapolation distances can be reasonably put at less than $\pm 1\%$. The main causes of a deviation of k_{eff} (static) from true k_{eff} are therefore errors in δ_x , δ_y , and M^2 . It can be shown, assuming errors in B_z^2 and κ^2 are negligible, that the fractional error in k_{eff} is given by

$$\frac{\Delta k_{\text{eff}}}{k_{\text{eff}}} = \left(B_z^2 + \kappa^2 \right) \frac{M^4 \Delta B_r^2 - \Delta M^2}{[1 + M^2(B_r^2 + B_z^2)][1 + M^2(B_r^2 - \kappa^2)]}$$

Thus, as the true multiplication of the array approaches 1.0 (i.e., as κ^2 approaches $-B_z^2$) the fractional error in k_{eff} (static) approaches zero.

Pulsed Measurements

In the pulsed measurements, the neutron source was a Texas Nuclear double-pulsed, 150-kv accelerator utilizing the $^3\text{H}(d,n)^4\text{He}$ reaction to produce 14-Mev neutrons. For the experiments with castings, the accelerator was situated with the tritium target about 180 cm above the top of the fuel as shown in position A of Figure 3. For the experiments with extrusion logs, the accelerator was moved to position B. In both cases two fully enriched $^{10}\text{BF}_3$ thermal neutron detectors were mounted parallel to the axis of the tank, usually at one-third and two-thirds of the estimated extrapolated pile height.

Standard neutron amplification and discrimination techniques for proportional counters were used with both detectors. A multichannel analyzer was operated in the multiscaling mode to simultaneously record the output of the detectors as function of time following the injected burst. The dead time imposed by the signal routing system for simultaneous storage of data was about 12.8 μsec . Peierls' statistical method¹⁰ was used to determine the persisting mode decay constant from the die-away.

The decay constant calculation was performed only with data accumulated after times longer than that required to establish the persisting mode. Experiments were performed to measure these times. A single $^{10}\text{BF}_3$ detector was mounted on the apparatus used to move the ion chamber in the static axial traverse measurements described earlier. One representative lattice of castings and one of extruded

logs were pulsed with the detector at various depths. The times required to establish the persisting modes were then obtained from plots of the prompt neutron axial distributions versus time.

The pulsed neutron experiments, analyzed with methods developed by Gozani,¹¹ Garellis-Russel,¹² and Sjöstrand,¹³ measured the reactivity in dollars, \$, a quantity directly proportional to the subcritical reactivity and independent of calculated parameters. The multiplication constant was then determined by

$$k_{\text{eff}} = \frac{1}{1 - (\$ - \beta_{\text{eff}})} \quad (6)$$

where β_{eff} is the effective delayed neutron fraction.

When the fundamental decay constant could be clearly identified, the averaging procedure suggested by Gozani¹⁴ was used to determine the \$ value for Equation (6):

$$\$(\text{avg}) = [$(\text{Gozani}) + $(\text{Garellis-Russell})]/2 \quad (7)$$

This method minimizes the effects from harmonic distortion of the spatial distributions of delayed neutrons. k_{eff} was also determined from the Sjöstrand value, and in cases where the fundamental decay constant could not be clearly identified, only the Sjöstrand value was used. However, deviations of \$ (Sjöstrand) from the true value can be anticipated because of uncorrected harmonic distortion. These distortions [and therefore the errors in \$(\text{avg})\$ and \$(\text{Sjöstrand})\$] should be minimized as k_{eff} approaches unity. A brief summary of procedures used to reduce the effects of harmonic distortion is given in Appendix A.

The determination of the effective delayed neutron fraction β_{eff} for small reflected systems is not straightforward. However, Gozani¹⁵ has shown that β_{eff} of the i^{th} delayed group can be approximated in the continuous slowing down model. In his treatment the delayed neutron importance function for the i^{th} group is

$$\gamma_i \equiv \beta_{\text{eff}_i} / \beta_i = e^{[B_g^2(\bar{\tau} - \bar{\tau}_i)]} \quad (8)$$

where $\bar{\tau}_i$ is the average slowing down area of the i^{th} group of delayed neutrons, and $\bar{\tau}$ is the average slowing down area of the total neutron spectrum. If variations in $\bar{\tau}_i$ from group-to-group are neglected, $\beta_{\text{eff}_i} / \beta_i$ is approximately the ratio of the nonleakage probability of the delayed groups to the nonleakage probability of the total spectrum. The ratio was calculated with S_n codes and sixteen-group Hansen-Roach¹⁶ cross sections. The calculations are described in Appendix B.

RESULTS

The experimental and calculated parameters determined for the rectangular lattices are summarized in Tables II and III. The first lines contain the measured parameters and an estimate of the experimental error. The quoted error on κ^2 measurements is the experimental precision. The error on the $\$$ (avg.) value is half the difference between $\$$ (Gozani) and $\$$ (Garelis-Russell). The next line tabulates the ratio $\beta_{\text{eff}_1}/\beta$ which was used to calculate k_{eff} (pulsed) from the measured dollar reactivities.

TABLE II

Calculated and Experimental Results for Castings in Water

Square Pitch, cm → Lattice →	20.1		20.7		21.3		22.0		22.6	
	2 x 2	2 x 3	2 x 2	2 x 3	2 x 2	2 x 3	2 x 2	2 x 3	2 x 2	2 x 3
<u>Measured Parameters</u>										
κ^2 (static), m^{-2}	10.55 ±.50	-1.80 ±.50	8.65 ±.50	-2.65 ±.50	8.70 ±.80	-3.30 ±.30	9.05 ±.50	-2.40 ±.30	10.10 ±.50	.10 ±.30
$\$$ (pulsed)										
Avg		-5.00 ±.39		-3.05 ±.10		-2.60 ±.02		-3.27 ±.14		-5.40 ±.03
Sjöstrand	-14.3	-4.77	-12.8	-2.92	-11.8	-2.58	-10.3	-3.09	-11.1	-4.47
<u>Calculated Parameters</u>										
β_{eff}/β	1.155	1.129	1.145	1.120	1.138	1.114	1.131	1.108	1.127	1.102
B_m^2 , m^{-2} (MGBS)	70.61		72.96		71.66		67.11		59.85	
M^2 , 10^{-4} m^2 (MGBS)	69.87		65.10		61.28		58.20		55.72	
<u>Calculated Reactivity</u>										
k_{eff} (MGBS-TGAN)	1.015	1.087	1.032	1.101	1.032	1.098	1.019	1.080	.996	1.052
k_{eff} (KEND)	.937	1.001	.950	1.026	.921	.982	.951	1.006	.944	.996
<u>Measured Reactivity</u>										
k_{eff} (static)	.921	.978	.933	.983	.935	.987	.937	.983	.933	.973
k_{eff} (pulsed)										
Avg		.965		.978		.982		.977		.963
Sjöstrand	.903	.966	.913	.979	.920	.982	.930	.978	.925	.969

TABLE III

Calculated and Experimental Results for First Extrusion Logs in Water

Square Pitch, cm → Lattice →	12.3		12.9			13.5		14.2	
	<u>2 x 3</u>	<u>3 x 3</u>	<u>2 x 2</u>	<u>2 x 3</u>	<u>3 x 3</u>	<u>2 x 3</u>	<u>3 x 3</u>	<u>2 x 3</u>	<u>3 x 3</u>
<u>Measured Parameters</u>									
κ^2 (static), m^{-2}	34.20 ±1.00	9.25 ±.30	58.00 ±2.00	31.75 ±2.00	6.53 ±.20	32.50 ±1.00	8.05 ±.30	35.75 ±1.00	11.88 ±.30
$\$$ (pulsed)									
Avg		-8.33 ±.42			-7.46 ±.31		-7.79 ±.34		-9.98 ±.58
Sjöstrand	-20.9	-7.86			-7.07	-20.2	-7.41	-22.0	-9.84
<u>Calculated Parameters</u>									
β_{eff}/β	1.153	1.122			1.113	1.135	1.106	1.128	1.099
B_m^2 , m^{-2}	87.88			86.66		83.62		74.01	
M^2 , 10^{-4} m (MGBS)	42.19			40.84		39.86		39.18	
<u>Calculated Reactivity</u>									
k_{eff} (MGBS-TGAN)	.928	1.011	.879	.948	1.030	.951	1.028	.939	1.012
k_{eff} (KENO)	.870	.955		.878	.966	.867	.946	.875	.956
<u>Measured Reactivity</u>									
k_{eff} (static)	.885	.952	.831	.892	.960	.890	.956	.880	.944
k_{eff} (pulsed)									
Avg		.943			.949		.947		.933
Sjöstrand	.865	.946			.951	.870	.949	.861	.934

MGBS⁵ is a multigroup code for computing the material buckling of fissile material moderated by water in an infinite, uniform configuration. This code contains its own internal set of 12-group cross sections for isotopes commonly found in reactors and processing plants, and is written such that wherever approximations are made they cause calculations to be more conservative in k_{eff} . Among other parameters, its output includes the material buckling B_m^2 , the migration area M^2 , and two group parameters for diffusion theory calculations. These latter parameters are used in a one-dimensional code TGAN⁵ that, among other things, calculates extrapolation distances into the reflector. A radial buckling is then computed using Equation (2), and the effective multiplication constant is obtained from Equation (3). The results of these calculations are tabulated as k_{eff} (MGBS-TGAN) for the arrays considered.

KENO⁶ is a multigroup Monte Carlo criticality code used at Savannah River with the 16-group Hansen-Roach cross section set.¹⁶ The output consists of k_{eff} and an estimate of its standard deviation plus a group-wise edit of leakage, absorption, and fission. The calculations, reported as k_{eff} (KENO), were performed assuming an H₂O reflector completely surrounded the arrays; the adjoint biasing technique¹⁷ was used to estimate neutron worths in the reflector. Although the experiments were run with no top reflector, its worth was calculated with KENO to be less than +0.005 in k_{eff} . The statistical error estimates for all KENO calculations were about ± 0.005 for 30,000 neutron histories.

MGBS values of M^2 and TGAN values of δ_x and δ_y together with appropriate values of κ^2 were used in Equation (4) to calculate the k_{eff} (static) given in Tables II and III. Values of k_{eff} (pulsed), using both \$ (Sjöstrand) and \$ (avg) where available, are also listed.

The measured quantities in Tables II and III can be used as experimental checks for other calculational methods. However, for those codes that determine only k_{eff} , such as KENO, the pulsed values determined from \$ (avg) are most appropriate since they do not rely heavily on calculated parameters and are most free of systematic error.

Figure 4 is a plot of the effective multiplication constants calculated with MGBS-TGAN as a function of the measured constants for the arrays of castings on a 20.7-cm pitch. This plot is typical of those encountered for both types of forms at all pitches. It shows systematic differences between the static and pulsed determinations of k_{eff} , differences due in part to the use of an

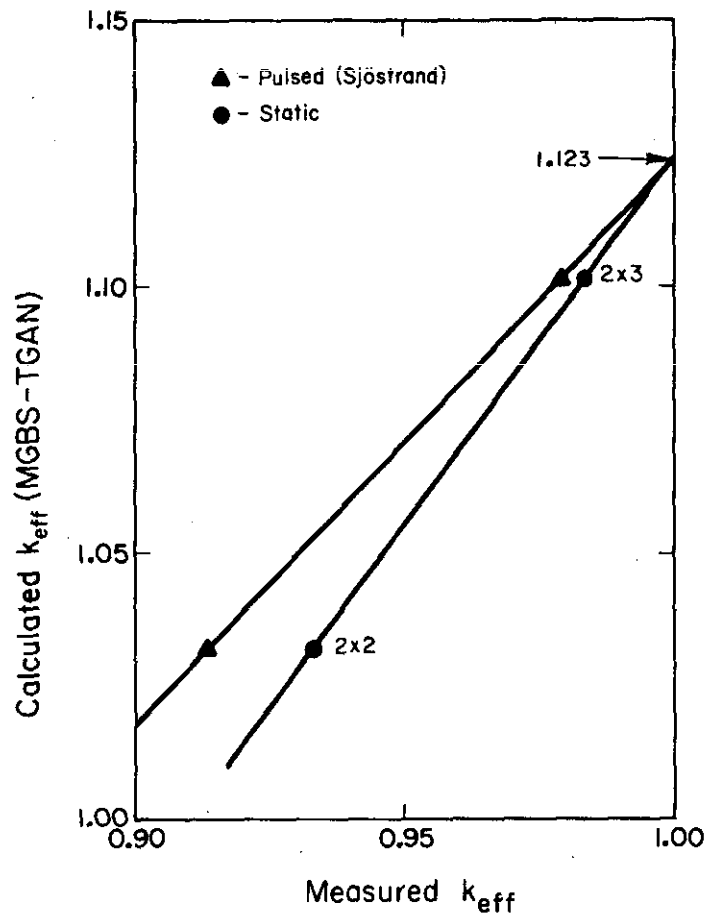


FIG. 4 COMPARISON OF CALCULATED AND MEASURED EFFECTIVE MULTIPLICATION CONSTANTS FOR CASTINGS ON 20.7-cm SQUARE PITCH

infinite lattice migration area in applying Equation (4) to these small systems and to the effects of harmonic distortions in the Sjöstrand analysis. The plot also shows that the results of the two methods appear to converge as the measured k_{eff} approaches unity. This is to be expected because, as has been shown, systematic errors in both techniques are minimized as k_{eff} approaches 1.0.

One quantity of interest in applying any criticality code is the value of k_{eff} that the code calculates for an exactly critical system. There are several ways of extracting this value from subcritical experiments. One method is to use plots of the type shown in Figure 4 to extrapolate subcritical measurements to criticality. Although the linear extrapolations are probably not

rigorous they seem adequate for estimating the conservatism of MGBS-TGAN at criticality, especially because, in all cases investigated, the two independent methods converge to the same value at criticality. Table IV summarizes this conservatism for the forms and pitches studies.

A second method often employed is to compute the ratio $k_{eff}(\text{calc})/k_{eff}(\text{meas})$. If the assumption is made that this ratio is constant as a function of $k_{eff}(\text{meas})$, then this constant is the calculated k_{eff} at criticality. The KENO calculations could be normalized in this fashion, but the available data indicate that the ratio is not constant as a function of $k_{eff}(\text{meas})$, probably because of inaccuracies in the measurements and the methods of analysis. As noted before, the k_{eff} value determined from the pulsed experiment bracketing procedure is most free from systematic error. Since \bar{k} (avg) values are available only for the most reactive arrays at each pitch, $k_{eff}(\text{KENO})/k_{eff}(\text{avg})$ for these arrays are summarized in Table IV as most representative of the conservatism of KENO at criticality for forms and pitches studies.

TABLE IV

Conservatism of Calculations

Form	Square Pitch, cm	MGBS-TGAN Conservatism ^a	KENO Conservatism ^b
Castings	20.1	1.120	1.037
	20.7	1.123	1.048
	21.3	1.116	1.000
	22.0	1.105	1.029
	22.6	1.091	1.034
Logs	12.3	1.068	1.011
	12.9	1.076	1.017
	13.5	1.078	1.017
	14.2	1.077	1.025

a. $k_{eff}(\text{calc})$ at $k_{eff}(\text{meas}) = 1.0$ by extrapolation of subcritical measurements.

b. $k_{eff}(\text{KENO})/k_{eff}(\text{avg})$ of most reactive lattice for each pitch and form.

Results of the 37 log experiments and the appropriate calculated values are given in Table V. The differences in the material buckling calculated with MGBS and that measured is about 13 m^{-2} . This difference corresponds to an error in k_{∞} of about 5% if the calculated value of M^2 is approximately correct.

Using the measured B_r^2 to determine the geometric buckling in k_{eff} (static) indicates that MGBS-TGAN calculations are in error by 4.4% in the calculation of k_{eff} . The results show that even in this large pitch case, the error in MGBS-TGAN calculations of k_{eff} is still quite large.

TABLE V
Results of 37 Log Measurements

$B_r^2, \text{ m}^{-2}$	$13.45 \pm .25$
$\kappa^2, \text{ m}^{-2}$	$9.28 \pm .25$
$B_m^2, \text{ m}^{-2}$	$4.17 \pm .35$
$k_{\infty} (\text{calc})/k_{\infty} (\text{meas})^a$	1.050
$B_m^2, \text{ m}^{-2}$ (MGBS)	17.18
$M^2, \text{ m}^2$ (MGBS)	38.84×10^{-4}
k_{eff} (MGBS-TGAN)	.986
k_{eff} (static)	.944
$k_{\text{eff}} (\text{calc})/k_{\text{eff}} (\text{meas})$	1.044
<hr/>	
a. $k_{\infty} = 1 + M^2 B_m^2$	

APPENDIX A

REDUCTION OF HARMONIC DISTORTION IN PULSED NEUTRON MEASUREMENTS

A convenient general representation of the time-dependent neutron density following a burst of source neutrons is an expansion in terms of the complete orthonormal set of kinetic eigenfunctions and eigenvalues. Within each mode, space and time are assumed to be completely separable. These modes can be described analytically only in the case of a bare homogeneous reactor.

Goarani¹¹ has given a two-group expression for the space and time dependence of neutron counts accumulated in a multiscaling channel at time θ after M pulses of period T .

where

$$N(r, \theta) = C \sum_{q=1}^{\infty} Q_q \phi_q(r) \sum_{j=0}^n A_{qj}(\gamma_{qj}, M, T) e^{\gamma_{qj}\theta} \quad (A-1)$$

C = constant independent of θ and r

Q_q = the q^{th} spatial component of the external source

$\phi_q(r)$ = the static geometric eigenfunctions

$A_{qj}(\gamma_{qj}, M, T)$ = constant independent of θ and r

γ_{qj} = the $(n+1)$ eigenvalues of the q^{th} two-group inhour equation. The γ value appropriate to the slowing down of fast neutrons to the thermal group is ignored. The eigenvalues γ_{q0} are the modal decay constants of the prompt thermal neutron dieaway; the γ_{qj} for $j > 0$ are due to delayed neutrons.

The detailed forms of the quantities in Equation (A-1) may be found in Reference 11.

Consider the Fourier eigenfunctions for rectangular geometries. In one dimension

$$\phi_q(x) = \sin\left(\frac{q\pi x}{X}\right)$$

where X is the extrapolated length of the reactor. A three-dimensional xyz representation would have

$$\phi_q(\vec{r}) \Rightarrow \phi_{klm}(\vec{r}) = \sin\left(\frac{k\pi x}{X}\right) \sin\left(\frac{\ell\pi y}{Y}\right) \sin\left(\frac{m\pi z}{Z}\right) \quad (\text{A-2})$$

Similarly for a cylindrical reactor with the source on the axis,

$$\phi_q(\vec{r}) \Rightarrow \phi_{kl}(\vec{r}) = \sin\left(\frac{k\pi z}{Z}\right) J_0\left(\frac{\alpha_\ell r}{R}\right) \quad (\text{A-3})$$

where the α_ℓ are the roots of the zeroth order Bessel function of the first kind.

The number of modes that can be minimized depends on the number and placement of detectors. From Equation (A-1) it can be seen that if a detector is placed at a point where $\phi_q(\vec{r}) = 0$, both the prompt and delayed neutrons in the q^{th} mode will not be recorded. At Savannah River two detectors are usually placed along an axis where the first nonfundamental eigenfunction in the transverse direction is zero. The detectors are then spaced at one-third and two-thirds the extrapolated reactor height. If the two detectors have equal efficiencies and their outputs are summed, the detected modes in rectangular lattices are: $k = 1, \ell = 1, m = 1$ (the fundamental); $k = 3, 5, 7, \text{etc.}; \ell = 3, 5, 7, \text{etc.}; m = 5, 7, 9$ etc. The even-order harmonics in k and ℓ disappear because of the transverse placement; in m they cancel because the even-order axial harmonic fluxes at the two detector positions are equal in magnitude but opposite in sign. In addition, the $m = 3$ harmonic disappears because the detectors are at the zeros of that harmonic.

Some knowledge of the magnitudes of the harmonic prompt neutron decay constants can be obtained by solving the Fermi age time-dependent problem in the absence of delayed neutrons:

$$\gamma_{q,0} = v\Sigma_a \left(1 + L^2 B_q^2 - k(1 - \beta) e^{-B_q^2 \tau} \right) \quad (\text{A-4})$$

where

L^2 = diffusion area

τ = Fermi age

In rectangular reactors, the buckling is

$$B_q^2 \Rightarrow B_{klm}^2 = \left(\frac{k\pi}{X}\right)^2 + \left(\frac{\ell\pi}{Y}\right)^2 + \left(\frac{m\pi}{Z}\right)^2$$

As the dimensions of the reactor grow larger, the buckling becomes smaller and the $\gamma_{q,0}$ values become more nearly alike. The larger the reactor, then, the more slowly the higher order harmonics will disappear, and the more difficult it will be to ascertain the prompt

fundamental decay free of harmonic distortion. Similarly, if L^2 and τ are small, the $\gamma_{q,0}$ values will be nearly alike, and it will be difficult to separate harmonic distortion from the prompt fundamental mode.

In the experiments of this report L^2 and τ were quite small, and the two detector technique was often not adequate to completely isolate the persisting prompt decay. Where this could not be done, the only recourse was to use the Sjöstrand method¹³ of analysis for β because it does not explicitly require a determination of the persisting mode decay constant. A correction for harmonic distortion was not attempted.

Where the persisting mode decay constant could be determined, both the Gozani and Garelis-Russell methods of analysis for β are valid. Gozani has shown that the delayed neutron eigenvalues (γ_{qj} , $j > 0$) hardly depend on the q modal index. "Therefore, the amount of delayed harmonics does not actually vary with time. However, since all delayed thermal neutrons belong to the second or to later generations of the source neutrons, they assume a distribution similar to the persisting one."¹¹ The small differences between the delayed and persisting distributions lead to different calculated values of β from the Gozani and Garelis-Russell methods of analysis. Gozani points out that these deviations from the true value of β are opposite in direction, though not necessarily equal in magnitude.¹⁴ For this reason, the bracketing procedure is recommended as tending to reduce further the effects of harmonic distortion.

APPENDIX B

METHOD FOR OBTAINING β_{eff}/β

More prompt neutrons than delayed neutrons leak from small reactors because the prompt fission distribution has a higher average energy. The delayed neutron fraction is thus effectively enhanced. Numerical computations of the enhancement can be made with any of several lattice and reactor codes. For the computations of this report, the S_n code ANISN¹⁸ was used along with the 16-group Hansen-Roach cross section library.¹⁶

The ANISN code will compute cell-homogenized cross sections for any number of groups. Cell calculations in cylindrical geometry were made for each lattice, and 4-group macroscopic cross sections were derived from the Hansen-Roach set. These cross sections were then used in two cylindrical reactor computations for each lattice. In the first, the fission energy distribution was that obtained by collapsing the 16-group Hansen-Roach set to 4 groups. Only groups 1 and 2 had nonzero populations. The second reactor computation used an artificial fission energy distribution where all the fission neutrons were born in group 2 (less than 0.9 Mev).

The value of β_{eff}/β was found by taking the ratio of the computed effective multiplication constants

$$\beta_{\text{eff}}/\beta = \frac{k(E_f < 0.9 \text{ Mev})}{k(E_f \text{ all energies})} \quad (\text{B-1})$$

since this is approximately the ratio of the nonleakage probability of the delayed neutrons to that of all fission neutrons. For one case the β_{eff}/β calculation was performed with 16 groups but the results were the same as with 4 groups.

REFERENCES

1. W. R. Stratton. "Correlations of Experiments and Calculations." *Proceedings Nuclear Criticality Safety*. USAEC Report SC-DC-67-1305, Sandia Corp., Albuquerque, N. M., p 91 (1966); also CONF-661206.
2. J. K. Fox, L. W. Gilley, and D. Callihan. *Critical Mass Studies, Part IX, Aqueous ^{235}U Solutions*. USAEC Report ORNL-2367, Oak Ridge National Laboratory, Oak Ridge, Tenn. (1958).
3. R. L. Hellens and G. A. Price. "Reactor-Physics Data for Water Moderated Lattices of Slightly Enriched Uranium." *Reactor Technology, Selected Reviews*. USAEC Report TID-8540, Argonne National Laboratory,
 H. K. Clark. *Critical and Safe Masses and Dimensions of Lattices of U and UO_2 in Water*. USAEC Report DP-1014, E. I. du Pont de Nemours & Co., Savannah River Laboratory, Aiken, S. C. (1966).
5. H. K. Clark. *Computer Codes for Nuclear Criticality Safety Calculations*. USAEC Report DP-1121, E. I. du Pont de Nemours & Co.,
6. G. E. Whitesides and N. F. Cross. *KENO: A Multigroup Monte Carlo Criticality Program*. USAEC Report CTC-5, Oak Ridge Gaseous Diffusion Plant, Union Carbide Corp., Oak Ridge, Tenn. (1969).
7. R. C. Axtmann and O. A. Towler. *The Savannah River Exponential Facility*. USAEC Report DP-49, E. I. du Pont de Nemours & Co., Savannah River Laboratory, Aiken, S. C. (1954).
8. R. C. Axtmann, L. A. Heinrich, R. C. Robinson, O. A. Towler and J. W. Wade. *Initial Operation of the Standard Pile*. USAEC Report DP-32, E. I. du Pont de Nemours & Co., Savannah River Laboratory, Aiken, S. C. (1953).
9. J. E. Woodward. *A Traveling Flux Monitor for Exponential Piles*. USAEC Report DP-659, E. I. du Pont de Nemours & Co., Savannah River Laboratory, Aiken, S. C. (1961).
10. R. Peierls. "Statistical Error in Counting Experiments." *Proc. Roy. Soc. A149*, 467 (1935).
11. T. Gozani. "The Theory of the Modified Pulsed Source Technique." *EIR Bericht Nr. 79* (1965).

12. E. Garelis and J. L. Russell, Jr. "Theory of Pulsed Neutron Source Measurements." *Nucl. Sci. Eng.* 16, 263 (1963).
13. N. G. Sjöstrand. "Measurements on a Subcritical Reactor Using a Pulsed Neutron Source." *Arkiv Fysik* 11, 233 (1956).
14. T. Gozani. "The Direct Measurability of Reactivity (In ρ) and Its Experimental Bounds (The 'Bracketing-Procedure')." *Trans Amer. Nucl. Soc.* 9, 274 (1966).
15. T. Gozani. "Subcritical Reactor Kinetics and Reactivity Measurements." *EIR Bericht Nr. 28* (1962).
16. G. E. Hansen and W. H. Roach. *Six and Sixteen Group Cross Sections for Fast and Intermediate Critical Assemblies.* USAEC Report LAMS-2543, Los Alamos Scientific Laboratory, Los Alamos, N. M. (1961).
17. G. E. Whitesides. "Adjoint Biasing in Monte Carlo Criticality Calculations." *Trans. Amer. Nucl. Soc.* 11, 159 (1968).
18. W. W. Engle, Jr. *A Users Manual for ANISN: A One-Dimensional Discrete Ordinates Transport Code with Anisotropic Scattering.* USAEC Report K-1693, Oak Ridge Gaseous Diffusion Plant, Union Carbide Corp., Oak Ridge, Tenn. (1967).